doi:10.1016/j.jmb.2009.02.026 J. Mol. Biol. (2009) 387, 809–825

JMB

Available online at www.sciencedirect.com

ScienceDirect

ELSEVIER

The Mouse Thymosin Beta15 Gene Family Displays Unique Complexity and Encodes A Functional Thymosin Repeat

Stien Dhaese[1,2], Klaas Vandepoele[3,4], Davy Waterschoot[1,2], Berlinda Vanloo[1,2], Joël Vandekerckhove[1,2], Christophe Ampe[1,2] and Marleen Van Troys[1,2]*

[1]*Department of Medical Protein Research, VIB, A. Baertsoenkaai 3, B-9000 Ghent, Belgium*

[2]*Department of Biochemistry, Ghent University, A. Baertsoenkaai 3, B-9000 Ghent, Belgium*

[3]*Department of Plant Systems Biology, VIB, Technologiepark 927, B-9052 Ghent, Belgium*

[4]*Department of Molecular Genetics, Ghent University, Technologiepark 927, B-9052 Ghent, Belgium*

Received 17 October 2008; received in revised form 10 February 2009; accepted 12 February 2009
Available online 20 February 2009

Edited by J. Karn

We showed earlier that human beta-thymosin 15 (Tb15) is up-regulated in prostate cancer, confirming studies from others that propagated Tb15 as a prostate cancer biomarker. In this first report on mouse Tb15, we show that, unlike in humans, four Tb15-like isoforms are present in mouse. We used phylogenetic analysis of deuterostome beta-thymosins to show that these four new isoforms cluster within the vertebrate Tb15-clade. Intriguingly, one of these mouse beta-thymosins, Tb15r, consists of two beta-thymosin domains. The existence of such a repeat beta-thymosin is so far unique in vertebrates, though common in lower eukaryotes. Biochemical data indicate that Tb15r potently sequesters actin. In a cellular context, Tb15r behaves as a *bona fide* beta-thymosin, lowering central stress fibre content. We reveal that a complex genomic organization underlies Tb15r expression: Tb15r results from read-through transcription and alternative splicing of two tandem duplicated mouse Tb15 genes. Transcript profiling of all mouse beta-thymosin isoforms (Tb15s, Tb4 and Tb10) reveals that two isoform switches occur between embryonic and adult tissues, and indicates Tb15r as the major mouse Tb15 isoform in adult cells. Tb15r is present also in mouse prostate cancer cell lines. This insight into the mouse Tb15 family is fundamental for future studies on Tb15 in mouse (prostate) cancer models.

Keywords: thymosin; actin; phylogeny; read-through transcript; qRT-PCR

Introduction

Beta-thymosins are either small proteins, consisting of approximately 40 amino acids, which are typically present in vertebrates, or longer variants with repeated units, which are present in lower metazoans.[1,2] The single unit vertebrate beta-thymosins are regarded as the main actin sequestering peptides.[3] By inhibiting the polymerization of bound monomeric actin, they influence the dynamic balance between filamentous and monomeric actin.[4] Recently, we clarified that three beta-thymosin isoforms are present in human, as has been described for the rat.[5] Thymosin beta4 (Tb4) and thymosin beta10 (Tb10) have already been characterized in several organisms.[6] We showed that one additional

*Corresponding author. Department of Biochemistry, Ghent University, A. Baertsoenkaai 3, B-9000 Ghent, Belgium. E-mail address: Leen.Vantroys@UGent.be.

Abbreviations used: EST, expressed sequence tag; eYFP, enhanced yellow fluorescent protein; F-actin, filamentous actin; G-actin, globular monomeric actin; ITC, isothermal titration calorimetry; NBD, 7-chloro-4-nitrobenzeno-2-oxa-1,3-diazole; qRT-PCR, quantitative real-time PCR; Tb4, thymosin beta4; Tb10, thymosin beta10; TbNB, neuroblastoma beta-thymosin; Tb15, thymosin beta15; Tb15r, thymosin beta15 repeat; TRAMP, transgenic adenocarcinoma of the mouse prostate.

isoform in humans, neuroblastoma beta-thymosin (TbNB), is the functional homologue of the previously reported rat thymosin beta15 (Tb15). This isoform has proved to be a promising biomarker for the early identification of prostate cancer patients at high risk of recurrence.[7] Tb15 has been reported to be up-regulated in breast, brain, lung and head and neck cancer.[8] The detailed molecular mechanisms underlying the role of Tb15 in cancer remain to be elucidated. Tb15/TbNB is reported to lower cellular filamentous actin content and stimulate cell migration upon over-expression.[5] Analogously, silencing rat Tb15 reduces cell migration.[9] Rat Tb15 has further been shown to have a pro-angiogenetic effect[10] and to promote neurite branching[11] and survival of motoneurons.[12]

Mouse Tb15-like isoforms have not been reported. Given that the mouse is an accepted model organism, in particular in the field of tumourigenesis, we undertook this study to unravel and characterize the mouse genes related to the human prostate cancer biomarker gene *Tb15*. We show that three Tb15-like gene loci encoding *bona fide* members of the Tb15-class are present in mouse. Next to a gene duplication that is commonly present in other mammals, an additional mouse-specific tandem duplication of a Tb15 locus has occurred. The three mouse Tb15 genes are transcribed separately but the tandem duplicated genes also give rise to a fourth, read-through, transcript resulting in an imperfect double repeat Tb15-like beta-thymosin (Tb15r). Biochemical characterization indicates that this longer Tb15r binds one actin monomer and displays unusually high sequestering activity. An extensive expression analysis of all mouse beta-thymosin isoforms (Tb4, Tb10 and new Tb15 isoforms) in adult mouse tissue and during embryonic development indicates, among other things, that Tb15r is the major Tb15 form in adult tissues.

Results

The mouse expresses more Tb15-like peptides than other mammalian species

To identify a murine thymosin beta15 (Tb15) homologue, we first used BLASTp (Basic Local Alignment Search Tool, Protein) at the NCBI website, searching with the human Tb15 amino acid sequence in the mouse RefSeq protein database†.[13] Unexpectedly, we found four different, but highly related Tb15-like peptide sequences predicted in this database (expectation value less than 10^{-13}) that are distinct from the known mouse thymosin beta4 (Tb4) and thymosin beta10 (Tb10). A multiple sequence alignment of these six mouse beta-thymosin forms demonstrates the high level of sequence conservation between all isoforms and, in particular, between the four newly identified proteins (Fig. 1a). Two of the Tb15-like sequences differ in only two amino acids. One of the Tb15-like forms is clearly atypical compared to the other vertebrate beta-thymosins with regard to its length: it is 80 amino acids long and contains two beta-thymosin modules (Pfam PF01290 or Prosite PS00500), therefore we called this peptide Tb15repeat or Tb15r (Fig. 1a).

To judge if we assigned the new mouse beta-thymosins to the Tb15 subclass correctly, we performed a protein sequence alignment and subsequent phylogenetic analysis of beta-thymosins of selected deuterostome species, available in public databases at present (for a list of sequences, see Supplementary Data S1). To evaluate how they relate to the mammalian beta-thymosins, we included single-domain beta-thymosins from urochordates and cephalochordates, which are at the origin of the vertebrate phylum.

The deuterostome phylogenetic tree shows that mammalian beta-thymosins are distributed mainly into three clusters (Fig. 1b), similar to our recent finding that the human beta-thymosin family is composed of three distinct protein isoforms; Tb4, Tb10 and Tb15.[5] Beta-thymosins from the cephalochordate amphioxus (*Branchiostoma belcheri* and *Branchiostoma floridae*) cluster at the base of the Tb15-clade, suggesting that Tb15 is at least as old as the divergence between cephalochordates and vertebrates between 810 and 1067 MYrs ago.[14] The four Tb15-like mouse isoforms clearly group together within the Tb15-clade, indicating that these peptides can indeed be categorized as Tb15 homologues. Interestingly, the rat also has two different Tb15-like peptides, whereas humans have only one Tb15 peptide sequence (see below).

Comparing the thymosin beta15 gene loci in human, mouse and rat reveals orthologous relationships and a mouse-specific duplication

It was reported recently that, although only one human Tb15 protein isoform is present, two different genes on chromosome X, *Tb15a* and *Tb15b*, encode this peptide.[8] Database inspection, including tBLASTn searches in the NCBI genomic database, indicated that the four mouse Tb15s newly reported here and the two rat Tb15s are also encoded by genes located on the X chromosome (Table 1). Surprisingly, the long mouse variant Tb15r maps to the same genomic location as two of the other isoforms, indicating that mouse has only three gene loci encoding four isoforms (see below).

To investigate the genomic conservation and organization of mouse *Tb15*-like gene loci, we performed a syntenic analysis, comparing the chromosomal maps of the regions on the X chromosome where the *Tb15* genes are located in human, mouse and rat (Fig. 2). For both *Tb15a* and *Tb15b*, multiple flanking genes are conserved between human and rat. On this basis, we named the two rat *Tb15* loci newly identified here *Tb15a* and *Tb15b*, according to the orthologous human loci. In mouse too, a *Tb15* gene is located in the region syntenic with that of human *Tb15a*. Interestingly, the region in mouse corresponding to human and rat *Tb15b* contains two

† http://blast.ncbi.nlm.nih.gov

adjacent Tb15-like encoding genes, indicating that a mouse-specific duplication event took place. We named these duplicated genes *Tb15b* and *Tb15c*, with respect to their order on the reverse strand of the X chromosome from which they are transcribed (Fig. 2). As pointed out above, the gene encoding the fourth atypically long mouse Tb15-like peptide covers both the *Tb15b* and *Tb15c* loci.

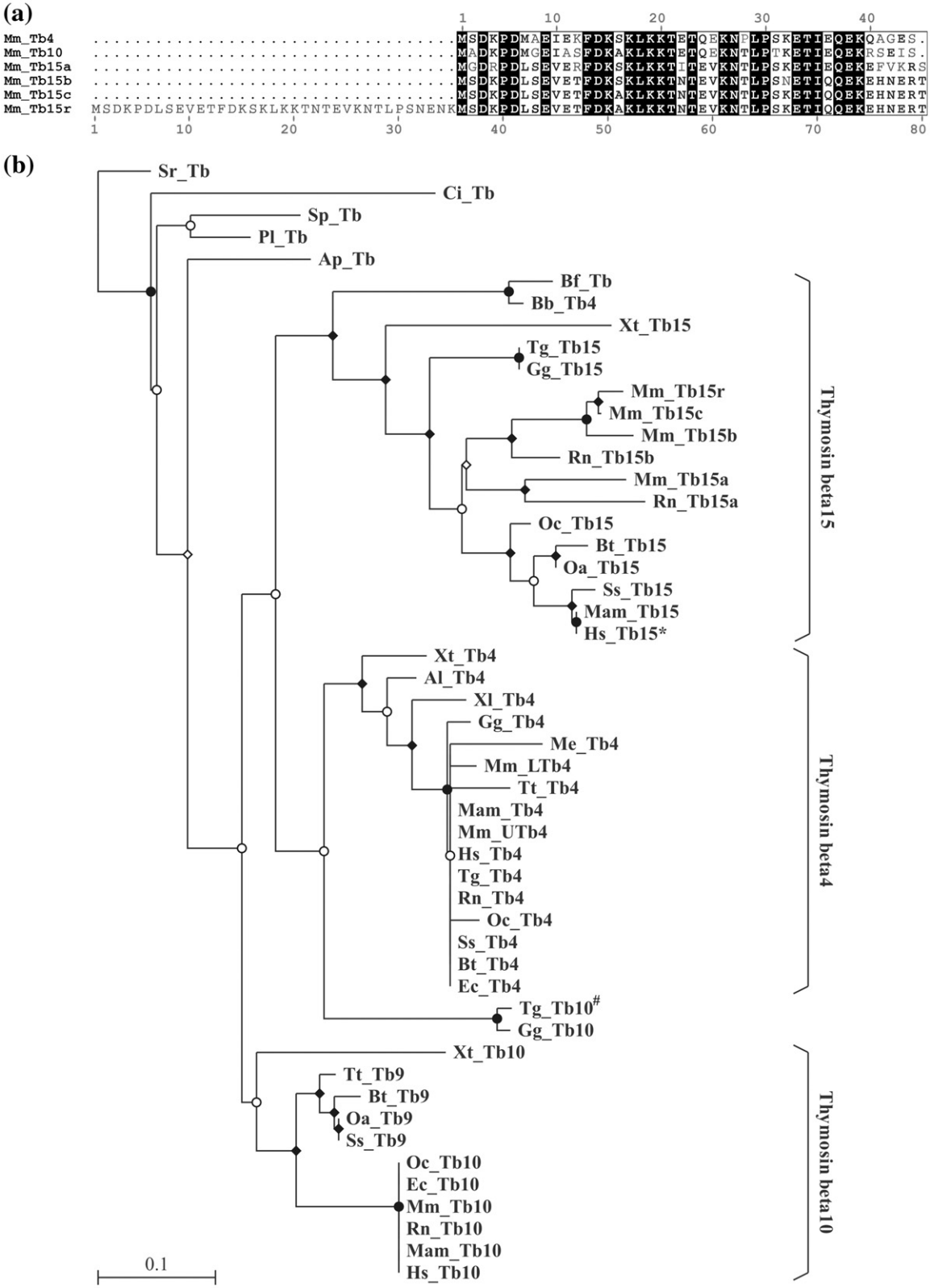

Fig. 1 (*legend on next page*)

Table 1. Genomic location of Tb15 gene loci in human, mouse and rat

	Gene name	Ensembl / NCBI gene ID	Chromosome band	Genomic location[a]
HsTb15a	TMSL8	*ENSG00000158164 / 11013*	Xq22.1	X:101655266-101658355(-1)
HsTb15b	TMSL8 (MGC39900)	*ENSG00000158427 / 286527*	Xq22.2	X:103105749-103107219(1)
MmTb15a	1700129I15Rik	*ENSMUSG00000060726 / 78478*	X-F1	X:132253206-132255212(-1)
MmTb15b	4930488E11Rik	*ENSMUSG00000072955 / 666244*	X-F1	X:133508561-133511413(-1)
MmTb15c	4930488E11Rik	*ENSMUSG00000079851 / 100034363*	X-F1	X:133489527-133492548(-1)
MmTb15r	4930488E11Rik	*ENSMUSESTG00000012724 / 399591*	X-F1	X:133489721-133511386(-1)
RnTb15a[b]	MGI:1925728	*ENSRNOG00000037661 / -*	Xq35	X:123022152-123023274(-1)
RnTb15b[c]	Tmsbl1	*- / 286978*	Xq35	X:101126074-101128188(-1)

Hs, *Homo sapiens*; Mm, *Mus musculus*; Rn, *Rattus norvegicus*.
[a] The genomic location on the assemblies NCBI_36.3 for human, NCBI_37.1 for mouse, RGSC _3.4 for rat *Tb15a* and Celera for rat *Tb15b*, is given as chromosome: gene_start_in_bp – gene_end_in_bp (strand_orientation).
[b] Not annotated in the NCBI database.
[c] The reference chromosome assembly in rat displays a gap at this position; however, the NCBI alternate assembly (based on Celera) covers this gap containing the annotated rat *Tb15b* gene.

Tandem duplicated mouse Tb15b and Tb15c genes are alternatively transcribed as one read-through transcript coding for a longer beta-thymosin with a repeated nature, Tb15r

If the two *Tb15b* and *Tb15c* genes, either separately or combined, give rise to the three predicted proteins Tb15b, Tb15c and Tb15r, then this should be evident from expressed sequence tag (EST) databases and/or from reverse-transcriptase PCR analysis on mouse tissues or cells. We used tBLASTn to search the mouse EST database at NCBI with mouse Tb15a, Tb15b, Tb15c and Tb15r protein sequences. This search yielded several specific ESTs for all forms, suggesting all the loci described above are actively transcribed and are not pseudogenes. Fewer ESTs were found for Tb15a and Tb15b (six and four, respectively) than for Tb15c and Tb15r (13 and 12, respectively) (Supplementary Data Table S3). Using primer sets for PCR-amplification of the different mouse beta-thymosin transcripts, we confirmed that transcription from the mouse *Tb15* loci occurs. This is demonstrated in Fig. 3 for mouse embryos at stage E14.5. Due to the high sequence conservation of Tb15b and Tb15c (96% sequence identity at the cDNA level), the primer set MmTb15b/c+r (Fig. 3a and b) does not distinguish between these forms and recognizes Tb15r, giving rise to two amplicons of different lengths (Fig. 3c). MmTb15r, the primer set specific for Tb15r, also resulted in a PCR product. This confirms the unique situation where the mouse *Tb15b/c* locus delivers a repeat beta-thymosin read-through transcript as well as separate transcripts (Fig. 3) (see qRT-PCR analysis, below).

By using BLAST for the coding sequences against the genomic sequence, we defined the exon–intron boundaries of the mouse *Tb15* genes (Table 2). The mouse *Tb15a*, *Tb15b* and *Tb15c* genes each have three exons; translation starts in exon 2 and stops in exon 3. The organization of the mouse *Tb15b* and *Tb15c* genes is depicted in Fig. 4a. Figure 4b shows the gene structures at the nucleotide level. Our prediction of organization and the size of exons and introns is in good accordance with the reported highly conserved gene structure of human, mouse and rat *Tb4*[15] (Table 2) and with the predicted exon–intron boundaries of the human and rat *Tb15* genes. The splice sites of the mouse *Tb15* genes strongly match the sequences of the consensus splice sites; a pyrimidine rich stretch and plausible branch-point can be located in each 3′ splice site (Fig. 4b).[16] The 3′ splice site that deviates

Fig. 1. Phylogenetic analysis, exploring the mouse Tb15 homologues. (a) Multiple sequence alignment of mouse beta-thymosins. Peptide sequences of mouse beta-thymosin isoforms: *Mus musculus* (Mm) Tb4, Tb10, Tb15a, Tb15b, Tb15c and Tb15r (GenBank accession numbers NP_067253, NP_079560, NP_084382, NP_001075452, NP_001074436 and NP_997150) were aligned using Multalin version 5.4.1;[52] the figure was generated with ESPript 2.2.[53] A high level of conservation is indicated in bold and highlighted in black. (b) Phylogenetic tree of beta-thymosins from selected deuterostoma species (see Materials and Methods for details on species selection and tree generation). The tree is based on the protein sequences available in Supplementary Data S1. The three main beta-thymosin clusters revealed by the phylogenetic analysis are indicated as thymosin beta15, thymosin beta4 and thymosin beta10. The beta-thymosins that were not yet annotated in public databases were named according to the cluster they group in. See the text for the naming of rat and mouse Tb15-like forms. The bootstrap values based on 1000 pseudoreplicates are represented as follows: open rectangle, ≤25%; open circle, >25% and ≤50%; filled rectangle, >50% and ≤75%; filled circle, >75%. Al, *Amolops loloensis*; Ap, *Arbacia punctulata*; Bb, *Branchiostoma belcheri*; Bt, *Bos taurus*; Ci, *Ciona intestinalis*; Cp, *Cavia porcellus*; Ec, *Equus caballus*; Gg, *Gallus gallus*; Hs, *Homo sapiens*; Mam, *Macaca mulatta*; Me, *Macropus eugenii*; Mm, *Mus musculus*; Oa, *Ovis aries*; Oc, *Oryctolagus cuniculus*; Pl, *Paracentrotus lividus*; Pr, *Poecilia reticulata*; Rn, *Rattus norvegicus*; Sp, *Strongylocentrotus purpuratus*; Sr, *Sycon raphanus*; Ss, *Sus scrofa*, Tg, *Taeniopygia guttata*; Tt, *Tursiops truncatus*; Xl, *Xenopus laevis*; Xt, *Xenopus tropicalis*. LTb4, lymphoid specific Tb4; UTb4, ubiquitous Tb4[54]; #Tg_Tb10 was named after Tb10 from chicken; *Hs_Tb15 peptide can be transcribed from two different highly similar genes (*Tb15a* and *Tb15b*).

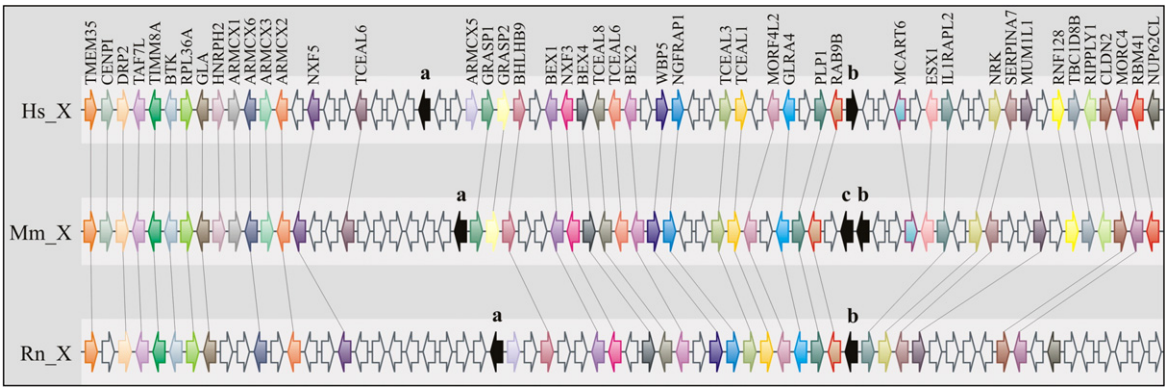

Fig. 2. Chromosomal mapping reveals tandem duplication of one of the two orthologous Tb15 gene loci in mouse compared to human and rat. Syntenic analysis of the regions of the human, mouse and rat X chromosome spanning the *Tb15* genes. The regions shown are: for human (NCBI_36.3 assembly) X:100220519-106336200 bp; for mouse (NCBI_37.1 assembly) X: 130829764-136533090 bp and for rat (RGSC_v3.4 assembly) X: 121773572- 128595524 bp. The gap in the rat RGSC_v3.4 assembly between 124528491 bp and 124736683 bp was filled with data from the rat Celera assembly overlapping this region. Genes are represented by arrows; arrows pointing to the left or right indicate transcription from the reverse or forward strand, respectively. Gene information was downloaded from the genomic database available at NCBI, only genes containing gene descriptions and geneIDs in the Ensembl database are retained in the figure. Colours indicate orthologous genes, based on the gene name (included in the figure) and gene description. For the genes indicated with an open arrow, no orthology can be indicated based on this information. Black arrows represent the different Tb15 genes, *Tb15a*, *b* and *c*, indicated by a, b and c.

(a)

PRIMER SET	PRIMER SEQUENCE 5′-3′	AMPLICON LENGTH (bp)
MmTb4	1. GACAAACCCGATATGGCT 2. CCTCATTACGATTCGCCAG	134
MmTb10	3. AGGAGAATCCACGAGTTGTAA 4. TTTCCTGTTCAATGGTCTCTTT	140
MmTb15a	5. TTGGTCTGATAGGTGGAGC 6. CCAGTGTTGGCATTTATTTGTTG	212
MmTb15b/c+r	7. CCAGAGGTAACTGTGGACATA 8. GTTCTTTCTCTTGCTGGATAGTTTC	181 (b/c) - 286 (r)
MmTb15r	7. CCAGAGGTAACTGTGGACATA 9. CGCTCATCTTGTTTTCATTCG	172

(c)

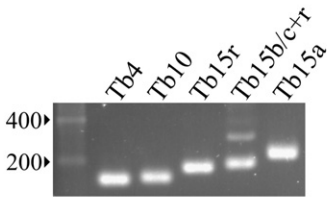

(b)

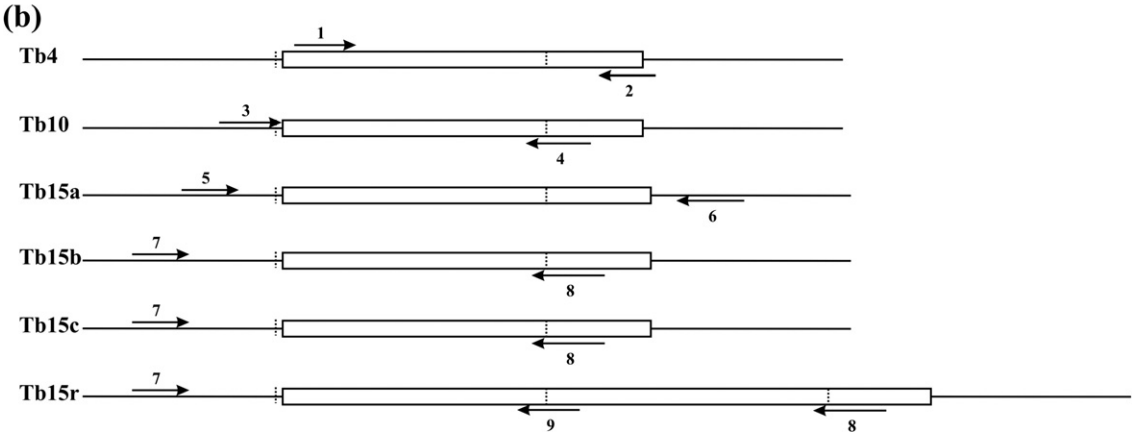

Fig. 3. Target specific PCR-based amplification of different mouse Tb15 isoforms. (a) The primer sequences of the five PCR primer sets used to detect mouse beta-thymosins and the length of resulting amplicons are summarized. (b) The location of each primer on the cDNA sequences of all mouse beta-thymosins is shown schematically. Coding sequences are boxed, forward (right-pointing arrow) and reverse (left-pointing arrow) primers are numbered in the scheme (b) as in the table (a). Exon boundaries are marked by vertical dotted lines. Two primer sets were used for Tb15r: forward primer 7 combined with reverse primer 9 amplifies part of the coding sequence that is specific for Tb15r (primer set specific for MmTb15r); primer 7 combined with reverse primer 8 amplifies part of the coding sequence that is shared by Tb15b, c and r (primer set MmTb15b/c+r). (c) qRT-PCR end products obtained from a sample derived from mouse embryos at embryonic stage E14.5 using primer sets MmTb4 (lane 1), MmTb10 (lane 2), MmTb15r (lane 3), MmTb15b/c+r (lane 4) and MmTb15a (lane 5) were separated on a 2% agarose gel. The amplicons have the expected length (see a). The primer sets depicted here were also used to generate the qRT-PCR data shown in Fig. 5.

Table 2. Organization of exons and introns is highly conserved between Tb4 and Tb15 genes from human, mouse and rat

	Genomic organization					Based on[a]		
	Exon 1 (bp)	Intron 1 (bp)	Exon 2 (bp)	Intron 2 (bp)	Exon 3 (bp)	Reference	Genomic contig (GenBank ID, selected region)	EST (GenBank ID)
Human *Tb4*	57	1076	116	409	448	15		
Mouse *Tb4*	56	1053	100	398	442	55, 56		
Rat *Tb4*	58	1000	115	396	432	57		
Human *Tb15a*	106	1485	117	939	443		NT_011651.16, HsX_11808:c25068007-25064919	NM_021992
Human *Tb15b*	97	1782	117	916	435	8	NT_011651.16, HsX_11808:c26513508-26516854	BC093093
Rat *Tb15a*	143	739	107	985	80		NW_001091921.1, RnX_WGA2841_4:c648586-650639	CR477043
Rat *Tb15b*	107	1208	105	494	215	58	NW_001091922.1, RnX_WGA2842_4:c430640-428512	CR477304, BM422866
Mouse *Tb15a*	121	1059	105	1252	216		NT_039716.7, MmX_39756_37:c9818766-9816764	BY707424, AV211171
Mouse *Tb15b*	121	1256	105	1158	216		NT_039716.7, MmX_39756_37:c11074976-11072121	DV065717
Mouse *Tb15c*	82	817	105	912	87		NT_039716.7, MmX_39756_37:c11056116-11053364	BU530212
	Exon 1 (bp)	Intron 1 (bp)	Exon 2 (bp)	Intron 2 (bp)	Exon 3 (bp)	Intron 3 (bp)	Exon 4 (bp)	Genomic contig (GenBank ID, selected region)	EST (GenBank ID)
Mouse *Tb15r*	121	1256	105	18,558	105	1252	216	NT_039716.7, MmX_39756_37:c11074976-11053364	BB667250

[a] Lengths and organization of exons and introns were summarized from the literature and/or exon–intron boundaries were predicted. Genomic sequences were outlined using the longest 5′UTR and 3′UTR sequences from ESTs obtained by a tBLASTn search of the beta-thymosin peptide sequences against EST sequence databases.

most from the consensus sequence is that of the last intron of *Tb15b*, where two adenines interrupt the pyrimidine tract (Fig. 4c).

As Tb15r and Tb15b are transcribed from the same promoter and use the same first two exons, they can be regarded as alternative splice products of the *Tb15b* gene. The Tb15r transcript, however, also uses exons from Tb15c, which renders the situation more complex (Fig. 4a). Indeed, the Tb15r read-through transcript contains exons 1 and 2 from *Tb15b* followed by exons 2 and 3 from the *Tb15c* gene interspaced by a large intron of 18,558 bp between both exon 2 sequences. The last exon from the *Tb15b* gene and the first exon from *Tb15c* are thus skipped (green boxes in Fig. 4a and b). Because the last exon of *Tb15b* is partly coding, the combination of *Tb15b* and *Tb15c* to *Tb15r* does not result in a perfect beta-thymosin repeat; the first unit of the repeat lacks the 12 amino acids that form the Tb15b C-terminus (Figs. 1a and 4b).

Tb15 isoforms are ubiquitously transcribed in adult mouse tissue, throughout development and in cell lines derived from prostate cancer

We quantitatively determined the transcript levels of all mouse beta-thymosin isoforms during development from embryonic stage E8.5 until E18.5, and investigated different adult tissues, including heart, kidney, liver, lung, muscle and spleen (Fig. 5).

During development in the mouse, all beta-thymosin isoforms except Tb15a display a similar temporal expression pattern, with *Tb10* being the most abundantly transcribed gene (Fig. 5a and b). Transcript levels of Tb4, Tb10 and the other Tb15s increase from embryonic stage E8.5 on, peak at E13.5 and diminish afterwards. Tb4 and Tb10 transcripts are approximately 200-fold more abundant than the Tb15 b/c and r transcripts, and this ratio between beta-thymosin isoform mRNA levels is constant throughout development. The Tb15a transcript levels are very low during all stages; approximately 100- to 200-fold lower than the other Tb15-like transcript levels (Fig. 5b). For stages E16.5 to E18.5, we separated head and body of the embryos (Fig. 5c and d). This revealed that whereas Tb15b/c and Tb15r transcript levels in the body are equal, in the head *Tb15b/c* display twofold higher levels than *Tb15r*.

In adult mouse organs, the situation is clearly different (Fig. 5e and f). In general, Tb4 is now the most abundantly transcribed isoform. The highest levels of Tb4 and Tb10 mRNA are observed in the spleen and lungs; the lowest levels are observed in striated muscle and the liver. Similar to embryos, the mRNA levels of the Tb15 isoforms are approximately one to three orders of magnitude lower than the Tb10 transcript levels. Of all mouse Tb15 isoforms, Tb15a again has the lowest transcript level, except in the heart, where it is the main Tb15 isoform present. In contrast to the embryonic stages, Tb15r is

now the main Tb15 isoform in most adult samples, reaching the highest levels in the spleen and lungs (Fig. 5f).

In general, beta-thymosin isoforms are difficult to detect with immunobased assays.[6] The 200-fold lower transcript levels of Tb15 compared to those of

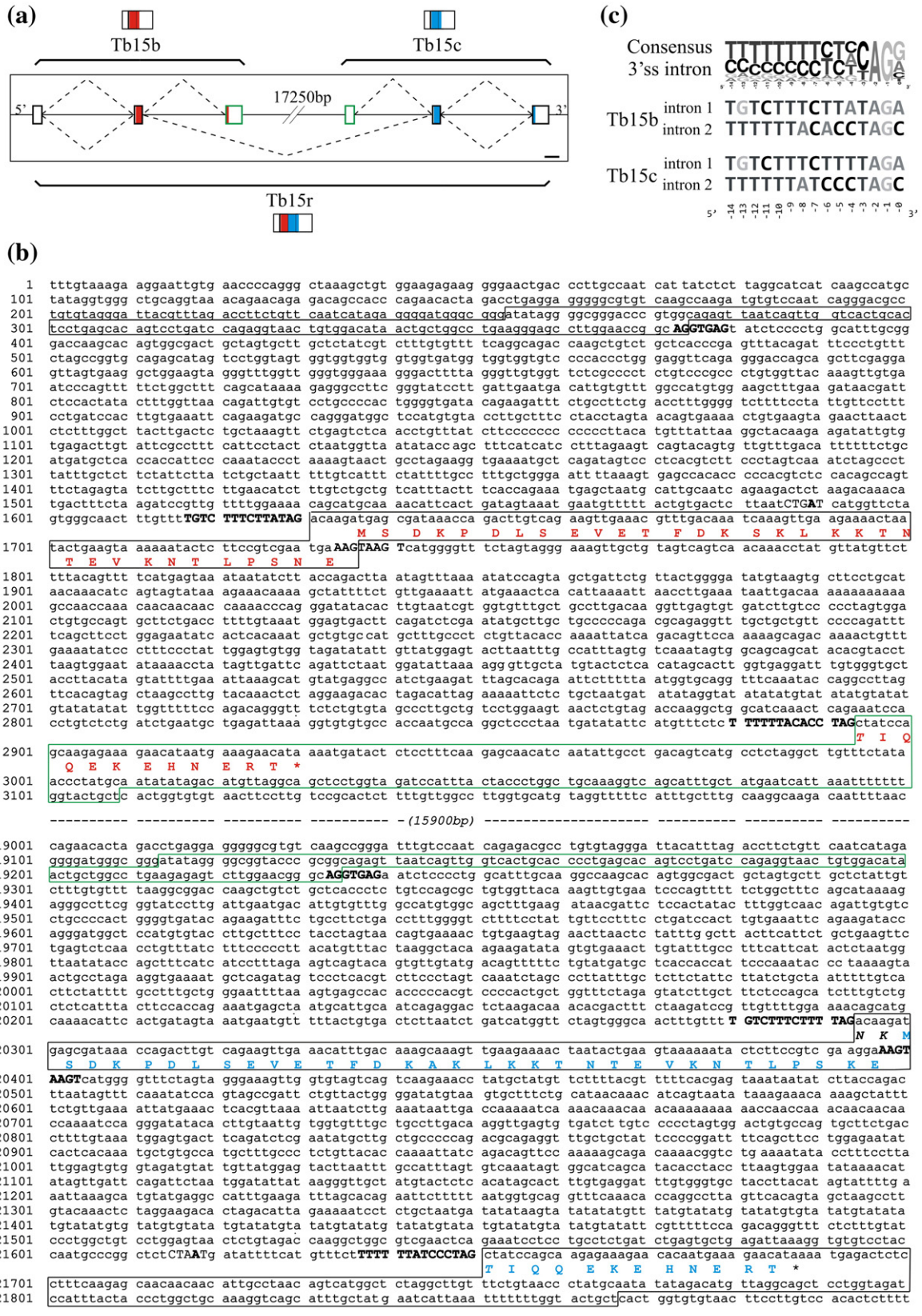

Fig. 4 (*legend on next page*)

Tb4 and Tb10 may explain why our attempts to detect these isoforms at the protein level have so far been unsuccessful (data not shown).

Since Tb15 expression has been correlated with prostate cancer,[9] we qualitatively analysed beta-thymosin expression in three cell lines derived from a primary prostate tumour of the transgenic adenocarcinoma mouse prostate (TRAMP) model.[17,18] Two of these cell lines, TRAMP-C1 and TRAMP-C2, are tumourigenic when grafted into syngeneic C57BL/6 hosts, whereas the third cell line, TRAMP-C3, is not.[17] Using endpoint reverse-transcriptase PCR, we demonstrate that, next to transcripts for Tb4 and Tb10, at least three Tb15 transcripts (Tb15a, Tb15b and/or Tb15c and Tb15r) are present in these three cell lines (Fig. 6).

Mouse Tb15r sequesters actin twice as strongly as its short counterpart Tb15c

Given the expression data described above indicating that Tb15r is the main Tb15 transcript in adult organs and is expressed in prostate cancer, it is important to understand the functional implication of its repeated nature. Real-time actin polymerization experiments demonstrate that Tb15r is more potent in inhibiting salt-induced actin polymerization compared to its short counterpart Tb15c (Fig. 7a). Adding 5 μM Tb15r to equimolar amounts of actin completely abrogates polymerization, whereas the same concentration of Tb15c allows some actin polymerization.

As a more quantitative approach, we used an actin sequestering assay with actin filaments with capped barbed ends. We derived equilibrium dissociation constants (K_d) of 1.4 μM and 0.7 μM for Tb15c–actin and Tb15r–actin complexes, respectively, confirming the stronger activity of Tb15r (Fig. 7b). By using isothermal titration calorimetry (ITC), we found a comparable K_d of 0.5 μM for the Tb15r–actin interaction (Supplementary Data Fig. S2). Note that the dissociation constant obtained for the mouse Tb15c–actin complex is already lower than those reported for Tb4 isoforms, conform earlier reports on human and rat Tb15.[5,19]

It has been shown that proteins with multiple beta-thymosin modules, e.g. *Caenorhabditis elegans* TetraThymosinβ[20] and *Drosophila melanogaster* CiboulotA,[21] can participate in the polymerization process by delivering actin monomers to free elongating barbed ends. Therefore, we tested if Tb15r is able to promote barbed end filament elongation; we performed the same experiment as above but in the absence of gelsolin, thus leaving barbed filament ends free (Fig. 7c).[20] Under these conditions, we obtained K_d values of 1.1 μM and 0.6 μM for Tb15c- and Tb15r–actin monomer complexes, respectively. These values are very close to those obtained when using capped barbed end filaments, indicating that Tb15r does not contribute to filament elongation. Note, furthermore, that Tb15r neither has a promoting effect on nucleation, a property described for other proteins containing consecutive actin monomer binding domains;[22,23] the lag phase in the polymerization curve is not shortened upon addition of Tb15r at any of the concentrations tested (Fig. 7a).

Taken together, our *in vitro* data show that the repeat beta-thymosin Tb15r is a pure actin-sequestering agent. Furthermore, Tb15r is twice as efficient as its short counterpart Tb15c in actin binding and sequestering.

Tb15r binds actin in a 1:1 complex

The calculated doubled affinity of mouse Tb15r *versus* Tb15c for actin monomers can result from two scenarios. Either Tb15r contains one functional actin binding module with a twofold higher affinity than the Tb15c actin-binding module, or Tb15r has two independent functional modules, both having affinities comparable to that of the single Tb15c module.

To discriminate between these two possibilities, we determined the stoichiometry of the actin–Tb15r complex. Titration of actin with Tb15r monitored by a band-shift assay in non-denaturing gels indicates that only one Tb15r-actin complex is formed (Fig. 8a). Zero-length chemical crosslinking of Tb15r to actin at various Tb15r:actin molar ratios followed by gel electrophoresis under denaturing conditions revealed that this complex has a molecular mass corresponding to one actin molecule and one Tb15r molecule (Fig. 8b).

Fig. 4. Tandem duplicated *Tb15b* and *Tb15c* genes are alternatively transcribed into Tb15repeat. (a) A representation of the genomic organization of the mouse *Tb15b* and *Tb15c* loci. Exons are boxed, the width of a box is drawn to scale compared to surrounding regions. The scale bar represents 200 bp. Filled boxes indicate coding regions and are coloured red for Tb15b and blue for Tb15c. Broken lines show the splicing strategy for each of the transcripts Tb15b, Tb15c (above) and Tb15r (below). Boxes close to the gene names represent the resulting spliced mRNAs, visualising that the Tb15r mRNA is composed of exons from both the *Tb15b* and *Tb15c* genes. Exons from *Tb15b* and *Tb15c* that are skipped for the Tb15r transcript are boxed in green. (b) Genomic sequence of the mouse *Tb15c* and *Tb15c* genes. Exon sequences are boxed. Splice sites and branching point consensus sequences are shown in bold, and/or in upper case. Asterisks indicate stop codons. Amino acid sequences encoded by *Tb15b* and *Tb15c* genes are shown in red and blue, respectively. For transcription of Tb15r, the exons boxed by a green line are skipped and the two residues unique to Tb15r (N and K at positions 33 and 34) as result of the fusion between exon2 from *Tb15b* and exon2 from *Tb15c* are shown in black. (c) Representation of the 3′ splice site (3′ss) intron consensus sequence compared to 3′ss intron sequences of mouse *Tb15b* and *Tb15c* genes. The consensus sequence was based on Ref. 16 and created with the web-based application WebLogo.

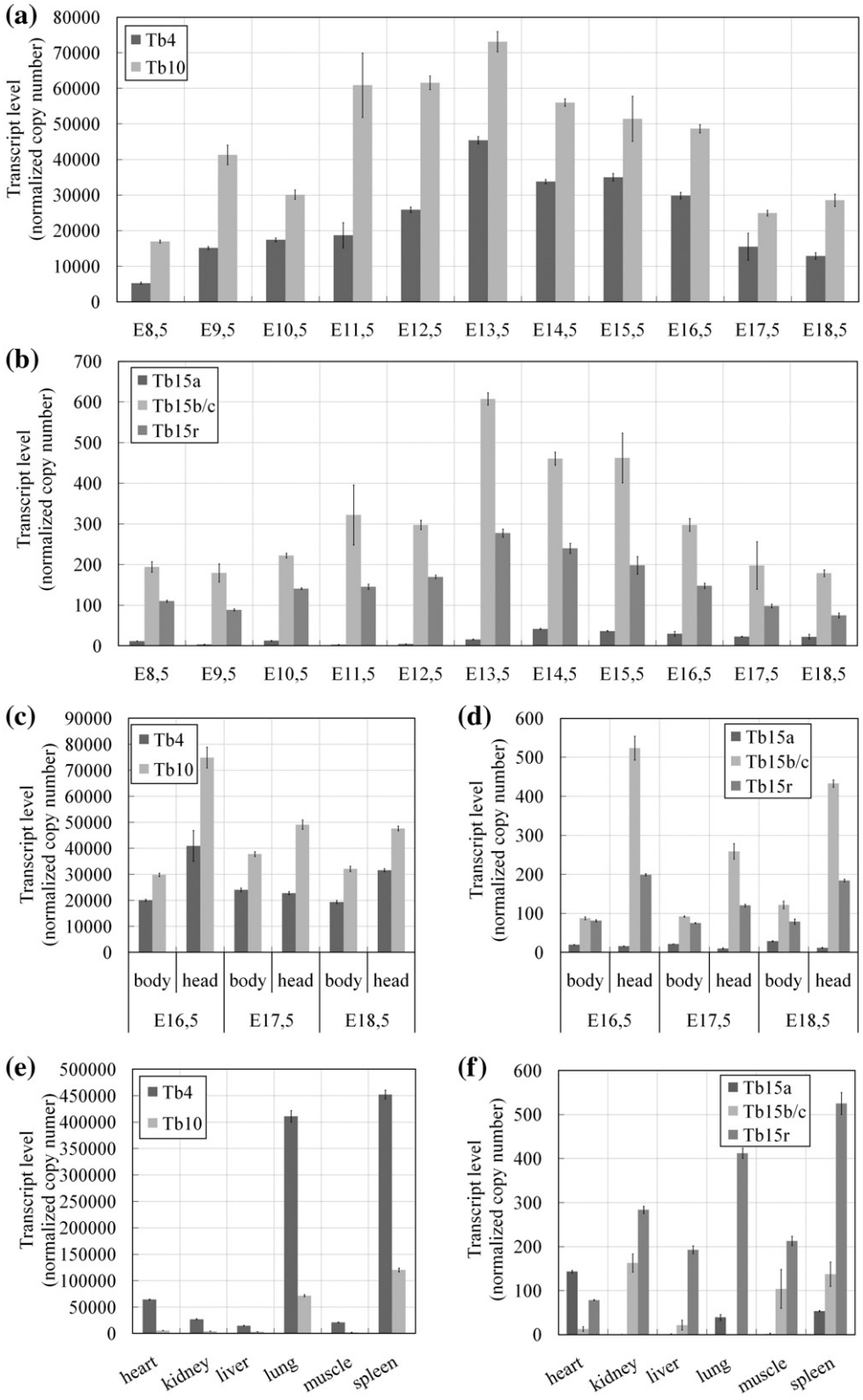

Fig. 5. Profiling of mouse beta-thymosins in stages of embryonic development and in adult organs. Absolute quantification results of qRT-PCR analysis of mouse beta-thymosins performed on samples from embryos of stage E8.5 to E18.5 (a and b), on samples from separated head and body of stage E16.5 until E18.5 (c and d) and on samples from adult heart, kidney, liver, lung, striated muscle and spleen (e and f). a, c and e show the normalized transcript copy numbers of mouse Tb4 and Tb10; b, d and f show the results for mouse Tb15a, Tb15b/c and Tb15r. Error bars represent standard deviations of mean values from duplicate samples.

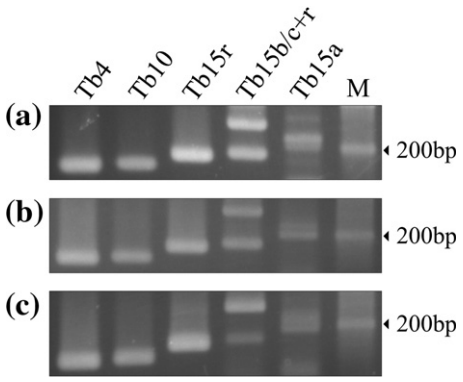

Fig. 6. Tb15 transcripts in mouse prostate cancer cell lines. Endpoint PCR on total cDNA from TRAMP-C1 (a), TRAMP-C2 (b) and TRAMP-C3 (c). Products were separated and visualized on a 2% agarose gel. Primer sets used are MmTb4 (lane 1), MmTb10 (lane 2), MmTb15r (lane 3), MmTb15b/c+r (lane 4) and MmTb15a (lane 5) (see Fig. 3a for primer sets and amplicon lengths). In all three TRAMP-C prostate cancer cell lines tested, at least three Tb15 isoforms are transcribed. M, marker.

A continuous variation experiment in which the total amount of protein (actin and Tb15r) was kept constant, showed a discontinuity at a molar ratio of 1.26:1.14 actin/Tb15r. This is the point where the maximum amount of complex is formed and thus reflects the stoichiometry of the complex. From two independent experiments, the mean value for the stoichiometry was calculated as 1.01 (±0.13) (Fig. 8c). ITC analysis also resulted in a value close to a 1:1 stoichiometry (Supplementary Data Fig. S2).

Tb15r strongly reduces actin fibers upon transient over-expression in mouse NIH3T3 fibroblasts

Over-expression of human Tb15 and other beta-thymosin isoforms in eukaryotic cells results in a reorganization of the actin cytoskeleton.[5] Using this approach, we compared the effect of mouse Tb15r and Tb15c. We found that cells transiently over-expressing Tb15r or Tb15c (fused to eYFP (enhanced yellow fluorescent protein)) both display a significant reduction in F-actin content compared to eYFP transfected control cells (Fig. 9a and b). Similar to what has been observed for human Tb15,[5] mainly central stress fibres are affected, whereas cortical actin bundles are still present. In addition, a perinuclear actin ring observed in non-transfected or in eYFP-expressing control cells was clearly absent from beta-thymosin over-expressing cells (Fig. 9a).

Discussion

During this study of the mouse homologue of the human Tb15, which is considered as a prostate tumour marker, we unexpectedly discovered the existence of additional Tb15 isoforms in mouse. Instead of the two *Tb15* gene loci present in human and rat, mouse has three loci encoding four

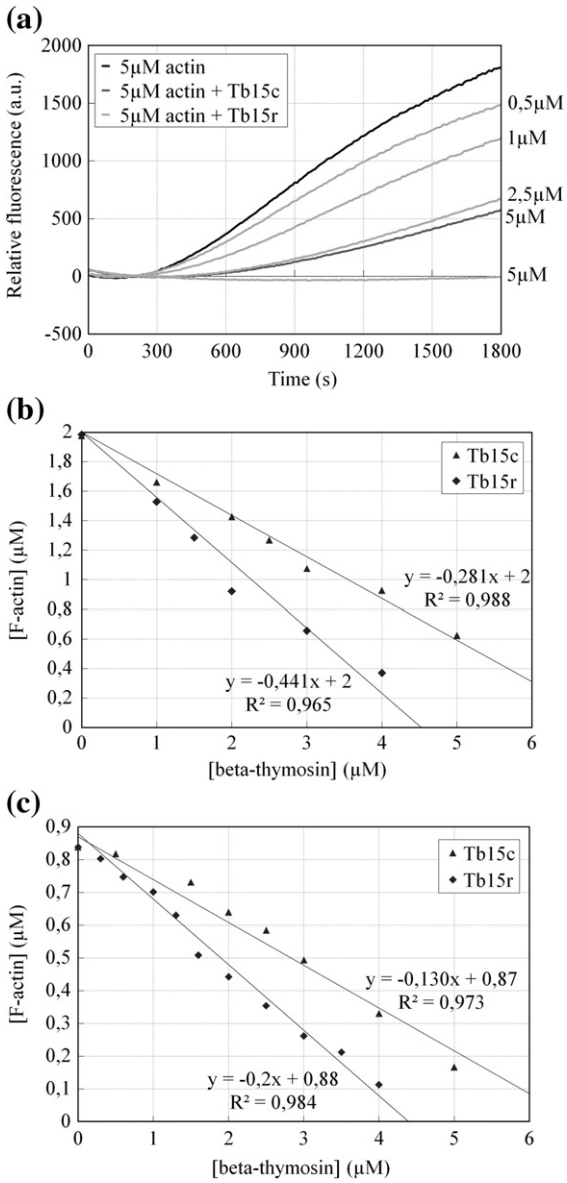

Fig. 7. Mouse Tb15r is twice as efficient in actin sequestering as Tb15c. (a) Kinetics of actin polymerization after addition of the indicated amounts of Tb15c or Tb15r to 5 μM actin (10% pyrene labelled) were monitored in real time by detecting changes in pyrene fluorescence as a measure of the amount of F-actin formed. (b and c) To quantify the actin monomer sequestering potential of Tb15c and Tb15r (represented by the decrease in F-actin), steady-state measurements of F-actin were done using either filaments with capped barbed ends (b) or filaments with free ends incubated with Tb15c and Tb15r at different concentrations (c). F-actin content at equilibrium was plotted as a function of beta-thymosin concentration. The K_d values for actin-Tb15c and actin-Tb15r complexes were derived from the slope: 1.4 μM and 0.7 μM, respectively, when barbed ends are capped (b, CMC of actin = 0.54 μM) and 1.1 μM and 0.6 μM respectively when filament ends are free (c, CMC of actin = 0.16 μM).

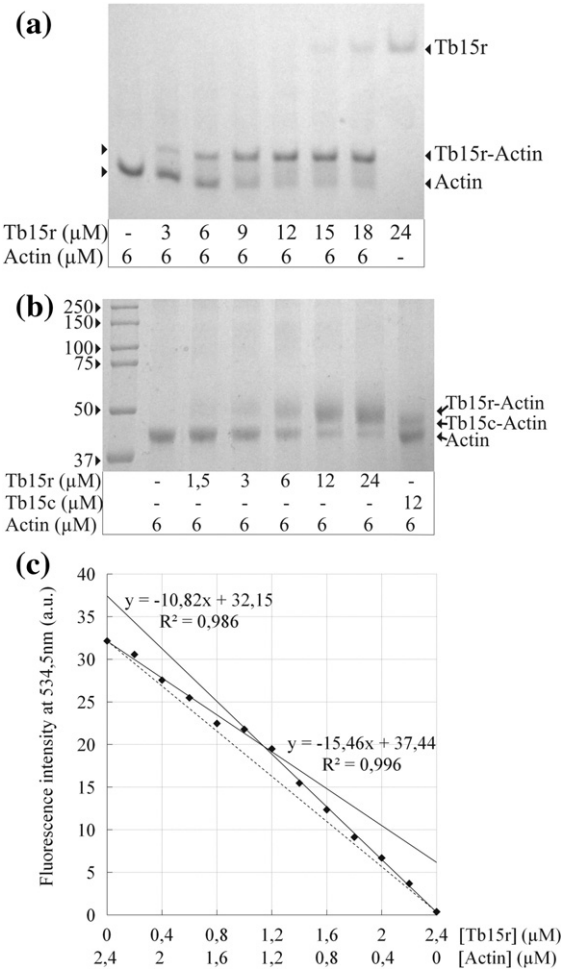

Fig. 8. Tb15r binds monomeric actin in a 1:1 complex. (a) Formation of the Tb15r–actin complex was monitored by non-denaturing gel electrophoresis indicating only one type of complex is visualized. (b) Zero-length cross-linking followed by denaturing gel electrophoresis and staining with Coomassie brilliant blue shows that this actin–Tb15r complex has a molecular mass of approximately 50 kDa, corresponding to one actin monomer (42 kDa) bound to one Tb15r molecule (8.8 kDa). (c) Fluorescence measurements of samples with various amounts of NBD-labelled actin and Tb15r at a constant total protein concentration (2.4 μM) revealed a transition point at 1.14 μM Tb15r and 1.26 μM actin (actin:Tb15r = 1.1). The broken line shows the theoretical fluorescence enhancement of actin alone.

different Tb15 isoforms. This unique situation is based on a mouse-specific gene duplication in combination with an intriguing read-through transcription of the duplicated genes. The latter gives rise to a fusion transcript encoding a functional mouse Tb15 double repeat that is twice as efficient as a single Tb15 in sequestering actin monomers *in vitro*. Moreover, an extensive tissue profiling analysis, comparing expression levels of all different mouse beta-thymosin isoforms, revealed that Tb15r is the main Tb15-like form expressed in most adult tissues. At least three different Tb15 transcripts, including Tb15r, are present in mouse prostate cancer cell lines. Future research on beta-thymosins in mouse (prostate) cancer models thus needs to take into account the different mouse Tb15-isoforms.

More than one Tb15 gene locus is generally present in mammals but in mouse, the complexity of the Tb15 gene locus additionally involves tandem duplication and read-through transcription

Phylogenetic analysis shows that the four newly reported mouse beta-thymosins are highly related Tb15 isoforms as they all cluster in the Tb15 clade. In addition, this analysis allows two novel conclusions contributing to the understanding of the beta-thymosin family. First, the three main clusters apparent in the presented phylogenetic tree provide a solid basis for a general classification of all mammalian beta-thymosins into three isoforms (Tb4, Tb10 and Tb15). This had been hypothesized on the basis of the fact that human as well as rat were reported to express three distinct beta-thymosin isoforms.[5] Second, the complexity of the Tb15 subfamily is clarified. More than one Tb15 form is present in mouse, and we reveal that two different Tb15-encoding transcripts exist also in rat, as was reported for human.[8] A syntenic analysis comparing mouse, rat and human further clarified that these two *Tb15* gene loci, *Tb15a* and *Tb15b*, must have existed in the common ancestor of rodents and primates (two *Tb15* loci are also predicted in Ensembl for chimpanzee and orang-utan). In accord with the orthologous relationships derived from the syntenic analysis, the mouse and rat *Tb15* gene products form a separate Tb15a and Tb15b cluster in the phylogenetic tree. This, however, cannot be observed for the human gene products, as these are identical. Since we showed that the duplication generating the *Tb15a/b* loci is not recent, the higher degree of sequence identity between human *Tb15a* and *Tb15b* than that between their respective orthologues in rat and mouse is intriguing and may suggest concerted evolution.

In mouse, one of the *Tb15* gene loci subsequently underwent a tandem duplication, resulting in two genes with separate promoters (b and c). In addition, we show the unique existence of a beta-thymosin read-through transcript spanning these two loci. Read-through transcription across the entire length of two neighbouring genes has been described in human, where 65 out of 41,919 transcriptional units were found to result from read-through transcription of two adjacent genes.[24] Because the underlying mechanisms of gene-combining read-through transcription remain to be elucidated, it is not clear whether we should consider these read-through transcripts as products of a new gene, or as alternative transcripts from the gene with which the promoter is shared. Although read-through transcription is reported to be a rare phenomenon, in this case it is used efficiently. The

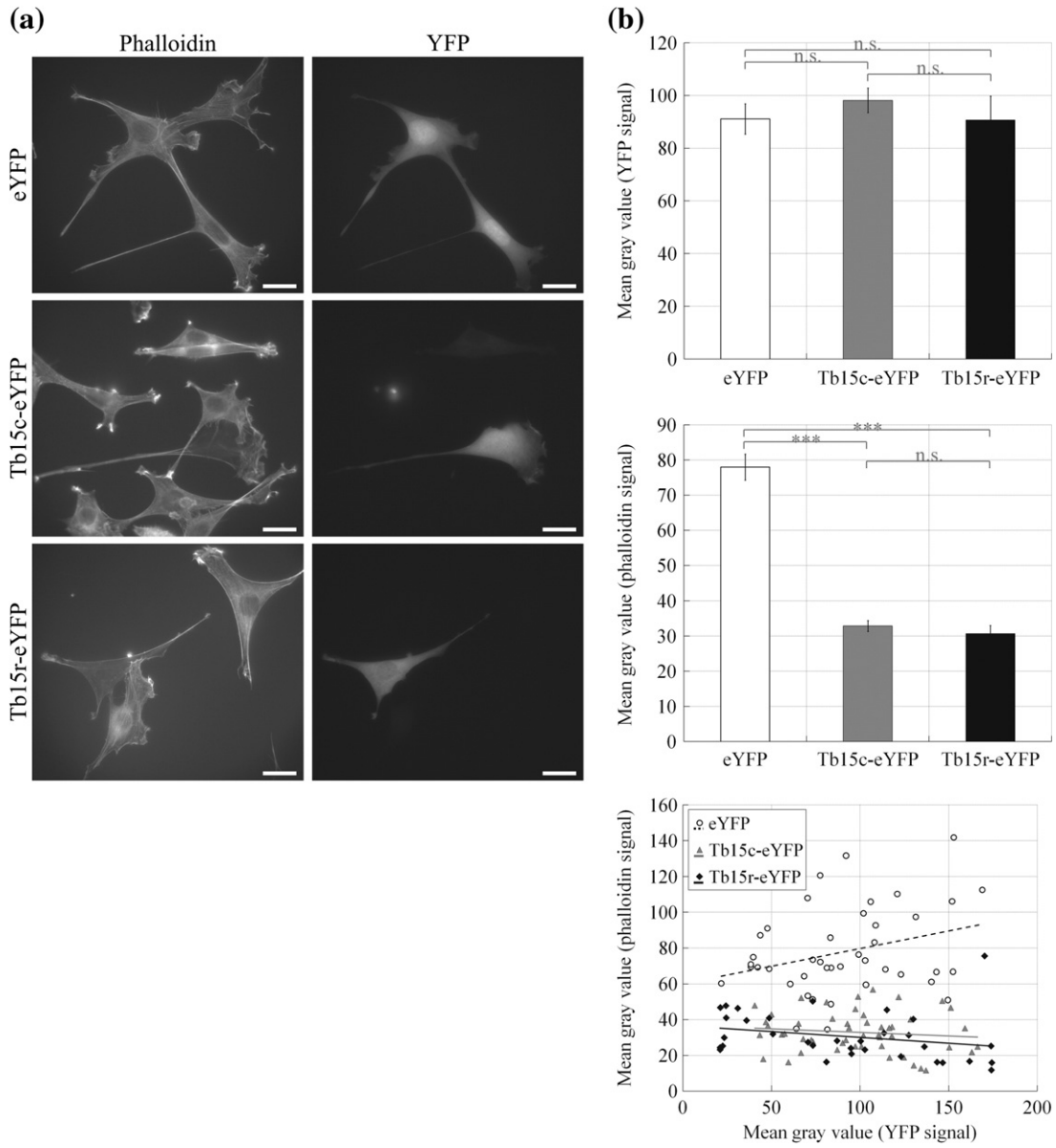

Fig. 9. Transient Tb15c and Tb15r over-expression in NIH3T3 affects the actin cytoskeleton. (a) Left-hand panels show the phalloidin signal (visualising cellular F-actin) and right-hand panels show the YFP signal (visualising expression of eYFP or eYFP-beta-thymosin fusions) in fixed NIH3T3 fibroblasts transiently expressing YFP, Tb15c-eYFP or Tb15r-eYFP. The scale bar represents 25 μm. (b) Quantitative analysis on cells from experiment shown in (a). The phalloidin and YFP signals were quantified by ImageJ as mean grey values of outlined cells. The number of cells analysed is 42, 52 and 33 for eYFP, Tb15c-eYFP and Tb15r-eYFP expressing cells, respectively. We selected cells with similar levels of over-expression, based on the YFP signal intensity (upper graph). Tb15c-eYFP and Tb15r-eYFP expressing cells show a similar, significant reduction in phalloidin signal compared to the control, eYFP expressing, cells (middle graph). Data are represented as mean±SEM. ***$p<0.0001$, $^{n.s.}p>0.25$ (not significantly different); the p-values were determined via Student's two-tailed t-test with Welch's correction. The reduction in F-actin is also evident from the scatter plot of the data (lower graph). Within the range of the selected cell population, no concentration-dependent effect of Tb15 expression on F-actin reduction is observed, since there is no correlation between the YFP signal and the phalloidin signal intensity (the slopes of the linear regression lines are not significantly different from zero, $p>0.05$).

Tb15r transcript is the major Tb15 form in adult organs. The switches in isoform expression of Tb15s during development (see also below) suggest regulation of this read-through mechanism. This is not unprecedented, the human DEC-205/DCL-1 fusion transcript was shown to have an expression pattern different from that of DEC-205 or DCL-1 alone, suggesting that read-through transcription of the two genes is differentially regulated compared to transcription of the single genes.[25] In case of Tb15r and Tb15b, differences in transcript regulation may be explained, in part, by the observed deviations from consensus in splice site sequences (Fig. 4c).

The mouse Tb15r has stronger actin sequestering activity

This work on Tb15r is the first report of a vertebrate beta-thymosin containing more than one beta-thymosin module (InterPro-domain 001152 or Pfam-domain PF01290). Despite the presence of these two putative actin-binding domains, we found that Tb15r binds only one actin monomer, albeit with a twofold higher affinity compared to its short, classical, counterpart Tb15c.

Studies on other beta-thymosin isoforms provide insight into the observed 1:1 stoichiometry of the Tb15r–actin complex. The beta-thymosin predicted modules that are present in Tb15r both contain the central hexapeptide motif (^{17}LKKTET[22] in Hs_Tb4) and the preceding hydrophobic patch (^{6}M, ^{9}I and ^{12}F in Hs_Tb4) which are crucial for actin binding by human Tb4.[26] The first module of Tb15r, however, differs from the second Tb15r module and from other single domain isoforms because it lacks 13 amino acids at the carboxy-terminus. A human Tb4 fragment with a similar 13 amino acid truncation was shown to have an activity 10-fold lower than that of full-length Tb4.[27] Additionally, a point mutation of a conserved residue in the C-terminus (I34A) lowered the affinity of the Tb4–actin complex more than 20-fold,[28] consistent with structural models indicating an interaction of the Tb4 C-terminal region with actin.[29,30] Collectively, this points to a significant contribution of the beta-thymosin C-terminus in actin binding. This predicts that the first module on its own would have low actin binding affinity and suggests that it is the second unit of Tb15r that is mainly responsible for Tb15r actin binding and sequestering. However, it does not fully explain why we find a 1:1 stoichiometry for Tb15r and actin. Indeed, we would still expect a 2:1 stoichiometry based on one weak and one strong Tb15r–actin interaction site. Possibly, steric hindrance may hamper simultaneous binding of two actin molecules. However, based on data from a mammalian protein with repeated beta-thymosin-related domains (Spire), the length between the two Tb15r units should be sufficient to allow binding of two actin monomers that have a head–tail orientation as in the actin filament.[22,31] Still, it is possible that the specific connection between the two Tb15r modules provokes conformational changes in Tb15r or induces a relative module positioning in Tb15r that sterically compromises the simultaneous binding of two actin monomers by Tb15r.

Under the assumption that actin binds to the second unit of Tb15r, it is evident that the first unit still has a favourable effect on the actin interaction of full-length Tb15r, since we observed that the actin binding affinity of Tb15r is doubled *versus* that of Tb15c (which is identical with the second Tb15r module). We speculate that the N-terminal part may have a stabilizing effect on the complex, thus lowering k_{off}. Alternatively, it cannot be excluded that the first unit could serve as an additional transient weak-affinity docking site for actin monomers, thereby multiplying the chance of interaction by increasing the local concentration of actin and in this way accelerating formation of the 1:1 complex of actin stably bound to the second Tb15r module by increasing k_{on}. Both effects could contribute to the observed lower equilibrium dissociation constant of the final 1:1 complex of actin with the repeat Tb15r *versus* that with the single domain Tb15c.

Although vertebrate beta-thymosins reported so far are all single-domain proteins, in lower eukaryotes and in protista several proteins have been described containing multiple copies of either beta-thymosin modules[20,21] or of the Wiskott-Aldrich syndrome homology 2 (WH2) domain, an actin-binding domain that is related to the beta-thymosin module.[22,23] These proteins do not simply behave as actin sequestering agents; they are able to promote actin nucleation or filament elongation. Models proposed to explain this rely on the fact that these proteins bind more than one actin molecule or may contact actin protomers in the filament. Our polymerization experiments, however, are consistent with the fact that Tb15r binds only one actin molecule, and consequently has no actin nucleation or filament elongation activity. Tb15r remains a pure actin monomer sequestering agent, albeit a more potent one, since its repeated nature renders it twice as efficient as a single beta-thymosin in maintaining a monomeric actin pool.

Isoform switching of mouse beta-thymosins in development and implications for exploring Tb15 as prostate tumour marker

We show that mouse Tb15 transcripts are present ubiquitously throughout mouse development (stage E8.5 until E18.5) and in various tested mouse adult organs, albeit at lower levels compared to those of the Tb4 and Tb10 isoforms. To our knowledge, relative levels of the three mammalian isoforms have been compared only in adult rat tissues using Northern blotting.[32] Consistent with our findings, this earlier study reported relatively large amounts of Tb4 and Tb10 mRNAs, but could not detect Tb15 in any of the organs examined. Our analysis reveals two isoform switches during mouse development; i.e. between expression in embryos and in adults. A first switch concerns the major isoforms Tb4 and Tb10, with Tb10 being the most abundant in the embryo and Tb4 being the most abundant in the adult. The Tb4 transcript profile we obtained in mouse adult tissue is in good accordance with a reported tissue expression profile of rat Tb4 at the protein level.[33] A second isoform switch occurs in the Tb15 family; compared to Tb15b/c, Tb15r is lower during embryogenesis whereas it is higher in adult organs. Importantly, we demonstrate that in the adult tissue set examined, with the exception of heart, Tb15r is the main Tb15 form expressed.

The switch in expression of the beta-thymosin isoforms suggests isoform-specific functions. This is especially relevant because beta-thymosins are reported to have a changed expression profile in many tumour types. Depending on tumour type, on

progression state or on other yet unknown factors, beta-thymosins are either up- or downregulated, and these changes are often restricted to a specific isoform.[34] To date, it remains unclear to what extent beta-thymosin isoforms are functionally redundant. They all appear to directly influence actin dynamics *in vitro* and in cells in a similar manner,[35,36] but opposing effects on angiogenesis and apoptosis have been described for Tb4 and Tb10.[37–39] Tb15 has been less well studied and has only recently gained attention because it was discovered to function as a biomarker for prostate cancer in human.[7] A preliminary study in prostate cancer patients indicated that Tb15 in combination with prostate-specific antigen (PSA) may increase the accuracy of prostate cancer diagnosis significantly.[40] Currently, an important strategy in prostate cancer research is the development and use of mouse models.[41] We detected both single and repeat Tb15 transcripts in TRAMP-C1 to 3. These mouse prostate cancer cell lines represent different tumour stages and are derived from an established and frequently used mouse model of prostate cancer.[17,18] Our data suggest that Tb15r, with its higher actin sequestering activity, may contribute to possible Tb15-related effects in mouse prostate cancer. Researchers studying the potential of Tb15 as biomarker using murine models should therefore consider the existence of different mouse Tb15 isoforms, including Tb15r. This underscores the significance of this report for ongoing and future cancer research.

Materials and Methods

Phylogenetic analysis

We retrieved protein sequences containing the thymosin beta4 family signature defined by Prosite entry PS00500 or Pfam entry PF01290 from the Swiss-Prot/TrEMBL database. The list was refined using evidence from the literature[2] and using results obtained by BLASTing the NCBI and Ensembl databases. We excluded beta-thymosins predicted solely on genomic DNA cloning data and focussed on beta-thymosins from deuterostome species. Because it is known that fish branched off early in the vertebrate evolution and thereafter underwent a fish-specific genome duplication,[42] we chose to omit beta-thymosins belonging to the class of Actinopterygii (including modern fish) from the phylogenetic tree in order to obtain a clear view on the mammalian beta-thymosin phylogenetic distribution. The finally selected protein sequences are given in Supplementary Data S1.

Sequences were aligned with Clustal W.[43] A neighbour-joining phylogenetic tree was constructed using TreeCon[44] based on Poisson corrected evolutionary distances, including a bootstrap analysis using 1000 replicates. The topology of the tree was confirmed with PhyML which uses the maximum likelihood instead of the neighbour-joining method.[43] We chose beta-thymosin from the sponge *Sycon raphanus* as an outgroup to root the tree.

Endpoint reverse transcriptase PCR

Briefly, cDNA was prepared from DNase I-treated total RNA isolated from flash-frozen mouse tissue and embryos (Swiss mice) or from collected TRAMP-C cells (RNeasy Midi (Qiagen), High Pure RNA Isolation kit (Roche), Transcriptor First Strand cDNA Synthesis kit (Roche)). Target specific primers were designed based on GenBank accession numbers NM_021278, EL959182, BU530212, DV065717, BU530212, BB667250 reported in *Mus musculus* for Tb4, Tb10, Tb15a, Tb15b, Tb15c and Tb15r, respectively, as documented in Fig. 3.

Quantitative real-time PCR (qRT-PCR) reactions on mouse tissues and embryos were done in duplicate on a LightCycler 480 (Roche) using the Fast start SYBR green master mix (Roche). We performed absolute quantification using external calibration curves generated with recombinant DNA. Dilutions ranging from $>10^7$ to <10 molecules/reaction were used for these curves. The combined copy number of Tb15b and Tb15c was quantified by subtracting the copy numbers obtained using primer set MmTb15r from those obtained using primer set MmTb15b/c+r. We normalized using a normalization factor calculated by qBASE software‡ that was based on qRT-PCR results of a set of housekeeping genes analysed for each sample. For embryonic tissues, the combination of glucose-6-phosphate dehydrogenase (G6PDH), hypoxanthine-guanine phosphoribosyltransferase (HPRT), phosphoglycerate kinase 1 (PGK1) and ubiquitin-C (UbC) as housekeeping genes resulted in the lowest variation of reference gene transcription levels across the samples. In adult tissues, we selected HPRT, PGK1 and UbC as a valuable set of housekeeping genes for normalization. (For full details, refer to Supplementary Data, Methods.)

Endpoint PCR on TRAMP-C cells was performed on equal amounts of cDNA using 0.5 μM forward and reverse primers and 2.5 units of Taq Polymerase (Invitrogen) in EasyStart™ PCR Mix (Mol. BioProducts); 42 rounds of amplification were done.

Recombinant expression of Tb15c and Tb15r peptides

Tb15c and Tb15r coding sequences were amplified from cDNA of mouse kidney tissue using forward primer 5′-GGCATATGAGCGATAAACCAGACTTG-3′ and reverse primer 5′-GGCCATGGTTATGTTCTTTCATTGTGTTC-3′ and cloned into the prokaryotic expression vector pET30a (Novagen) between the NcoI and NdeI (New England BioLabs) restriction sites. Proteins were expressed in BL21(DE3) cells after induction by isopropyl-beta-D-thiogalactopyranoside. Purification of beta-thymosin was done by adding four volumes of ice-cold 0.3 M perchloric acid to cleared cell lysate, followed by centrifugation to remove precipitated protein, neutralization of the supernatant with potassium chloride, centrifugation and final purification by C18 reverse-phase HPLC (Waters).[45] The correct molecular mass of reverse-phase HPLC-purified peptides was confirmed by mass spectrometry.

Actin binding assays

Rabbit skeletal muscle actin was prepared and stored in G-buffer (5 mM Tris–HCl pH 7.7, 0.1 mM $CaCl_2$, 0.2 mM ATP, 0.2 mM DTT).[46] Actin was labelled with *N*-pyrenyliodoacetamide[47] or with 7-chloro-4-nitrobenzeno-2-oxa-1,3-diazole (NBD).[48] The effect of beta-thymosin on actin polymerization kinetics, and the dissociation

‡ http://medgen.ugent.be/qbase/

constants of beta-thymosin–actin complexes were determined as specified.[5] Details of K_d calculations are described in Ref. 26 For conditions in which barbed filament ends are capped, we incubated F-actin with the barbed end capping protein gelsolin in a molar ratio of 200:1 actin/gelsolin before incubation with Tb15. The critical monomer concentration of actin (0.16 μM and 0.54 μM for filaments with free or capped barbed ends, respectively) was derived from parallel experiments.

Actin monomer binding of Tb15r was assayed using band-shift in non-denaturing PAGE,[49] using zero-length crosslinking as described,[50] or using NBD-labelled actin for a continuous variation experiment (the Job method) as adapted from Ref. 51 Briefly, NBD-actin and Tb15r were diluted in G-buffer and incubated at various molar ratios but at a constant total protein amount of 2.4 μM for 30 min at room temperature. Fluorescence spectra were obtained using excitation at 475 nm. The emission maximum was reached at 534.5 nm.

Beta-thymosin eukaryotic expression

Mouse Tb15c and Tb15r coding sequences were amplified from cDNA of mouse kidney tissue using forward primer 5′-CGCTCGAGATGAGTGATAAACCAGAC-3′ and reverse primer 5′-CGTGGATCCGCAGTTCTTTCATTGTGTTC-3′ and cloned into XhoI and BamHI (New England Biolabs) sites of mammalian expression vector pEYFP-N1 (Clontech, BD Biosciences) allowing expression of beta-thymosin C-terminally fused to eYFP. We transfected NIH3T3 cells using FuGene6 Reagent (Roche) with plasmid DNA (EndoFree Plasmid Maxi kit, Qiagen).

Cell culture and staining

NIH3T3 cells (ATCC) were cultured in Dulbecco's modified Eagle's medium (DMEM) with GlutaMAX™-I (Gibco) supplemented with 10% (v/v) heat-inactivated fetal bovine serum (Gibco) and 1% (w/v) penicillin-streptomycin (Gibco). Cells were cultured at 37 °C in a 5% (v/v) CO_2 atmosphere. Staining with phalloidin was as described.[5] Images of control and Tb15-eYFP fusion protein expressing cells were taken using identical microscope settings and fluorescence intensities were quantified by ImageJ software§. Statistical analyses were performed via GraphPad Prism 5 software.

TRAMP-C cell lines (C1,C2,C3) were obtained from ATCC and cultured at 37 °C in an 8% (v/v) CO_2 atmosphere in DMEM containing 4 mM L-glutamine, 4.5 g/l glucose without sodium pyruvate (Gibco) supplemented with 10% fetal bovine serum, 5 μg/ml bovine insulin (Sigma) and 10 nM 5-alpha-androstan-17beta-ol-3-one (Fluka).

Acknowledgements

We thank Jozef Vandamme for help with mass spectrometric analysis, Mark Goethals for assistance with HPLC purification, and Tine Blomme and Thomas Van Parys for help with Fig. 2. S.D. is a fellow of the Research Foundation - Flanders (Belgium) (FWO-Vlaanderen) and K.V. is a postdoctoral fellow of the Research Foundation - Flanders. This work was supported by FWO research grant G.O157.05 to M.V.T. and C.A., BOF research grant D1J04806 to M.V.T. and GOA grant 01G01207 to C.A. and J.V.

§ http://rsb.info.nih.gov/ij/

Supplementary Data

Supplementary data associated with this article can be found, in the online version, at doi:10.1016/j.jmb.2009.02.026

References

1. Van Troys, M., Vandekerckhove, J. & Ampe, C. (1999). Structural modules in actin-binding proteins: towards a new classification. *Biochim. Biophys. Acta*, **1448**, 323–348.
2. Van Troys, M., Dhaese, S., Vandekerckhove, J. & Ampe, C. (2007). Multirepeat beta-thymosins. In *Actin-Monomer-Binding Proteins* (Pekka, L., ed), 14th edit., pp. 71–81. Landes Bioscience, Austin, TX.
3. Sanders, M. C., Goldstein, A. L. & Wang, Y. L. (1992). Thymosin beta 4 (Fx peptide) is a potent regulator of actin polymerization in living cells. *Proc. Natl Acad. Sci. USA*, **89**, 4678–4682.
4. Safer, D., Elzinga, M. & Nachmias, V. T. (1991). Thymosin beta 4 and Fx, an actin-sequestering peptide, are indistinguishable. *J. Biol. Chem.* **266**, 4029–4032.
5. Dhaese, S., Jonckheere, V., Goethals, M., Waltregny, D., Vandekerckhove, J., Ampe, C. & Van Troys, M. (2007). Functional and profiling studies prove that prostate cancer upregulated neuroblastoma thymosin beta is the true human homologue of rat thymosin beta15. *FEBS Lett.* **581**, 4809–4815.
6. Hannappel, E., Huff, T. & Safer, D. (2007). Intracellular beta-thymosins. In *Actin-Monomer-Binding Proteins* (Pekka, L., ed), 14th edit., pp. 71–81. Landes Bioscience, Austin, TX.
7. Hutchinson, L. M., Chang, E. L., Becker, C. M., Ushiyama, N., Behonick, D., Shih, M. C. *et al.* (2005). Development of a sensitive and specific enzyme-linked immunosorbent assay for thymosin beta15, a urinary biomarker of human prostate cancer. *Clin. Biochem.* **38**, 558–571.
8. Banyard, J., Hutchinson, L. M. & Zetter, B. R. (2007). Thymosin {beta}-NB is the human isoform of rat thymosin {beta}15. *Ann. N.Y. Acad. Sci.* **1112**, 286–296.
9. Bao, L., Loda, M., Janmey, P. A., Stewart, R., Anand-Apte, B. & Zetter, B. R. (1996). Thymosin beta 15: a novel regulator of tumor cell motility upregulated in metastatic prostate cancer. *Nature Med.* **2**, 1322–1328.
10. Koutrafouri, V., Leondiadis, L., Ferderigos, N., Avgoustakis, K., Livaniou, E., Evangelatos, G. P. & Ithakissios, D. S. (2003). Synthesis and angiogenetic activity in the chick chorioallantoic membrane model of thymosin beta-15. *Peptides*, **24**, 107–115.
11. Choe, J., Sun, W., Yoon, S. Y., Rhyu, I. J., Kim, E. H. & Kim, H. (2005). Effect of thymosin beta15 on the branching of developing neurons. *Biochem. Biophys. Res. Commun.* **331**, 43–49.
12. Choi, S. Y., Kim, D. K., Eun, B., Kim, K., Sun, W. & Kim, H. (2006). Anti-apoptotic function of thymosin-beta in developing chick spinal motoneurons. *Biochem. Biophys. Res. Commun.* **346**, 872–878.

13. Altschul, S. F., Madden, T. L., Schaffer, A. A., Zhang, J., Zhang, Z., Miller, W. & Lipman, D. J. (1997). Gapped BLAST and PSI-BLAST: a new generation of protein database search programs. *Nucleic Acids Res.* **25**, 3389–3402.
14. Blair, J. E. & Hedges, S. B. (2005). Molecular phylogeny and divergence times of deuterostome animals. *Mol. Biol. Evol.* **22**, 2275–2284.
15. Yang, S. P., Lee, H. J. & Su, Y. (2005). Molecular cloning and structural characterization of the functional human thymosin beta4 gene. *Mol. Cell. Biochem.* **272**, 97–105.
16. Shapiro, M. B. & Senapathy, P. (1987). RNA splice junctions of different classes of eukaryotes: sequence statistics and functional implications in gene expression. *Nucleic Acids Res.* **15**, 7155–7174.
17. Foster, B. A., Gingrich, J. R., Kwon, E. D., Madias, C. & Greenberg, N. M. (1997). Characterization of prostatic epithelial cell lines derived from transgenic adenocarcinoma of the mouse prostate (TRAMP) model. *Cancer Res.* **57**, 3325–3330.
18. Greenberg, N. M., DeMayo, F., Finegold, M. J., Medina, D., Tilley, W. D., Aspinall, J. O. *et al.* (1995). Prostate cancer in a transgenic mouse. *Proc. Natl Acad. Sci. USA*, **92**, 3439–3443.
19. Eadie, J. S., Kim, S. W., Allen, P. G., Hutchinson, L. M., Kantor, J. D. & Zetter, B. R. (2000). C-terminal variations in beta-thymosin family members specify functional differences in actin-binding properties. *J. Cell. Biochem.* **77**, 277–287.
20. Van Troys, M., Ono, K., Dewitte, D., Jonckheere, V., De Ruyck, N., Vandekerckhove, J. *et al.* (2004). Tetra-Thymosinbeta is required for actin dynamics in Caenorhabditis elegans and acts via functionally different actin-binding repeats. *Mol. Biol. Cell*, **15**, 4735–4748.
21. Boquet, I., Boujemaa, R., Carlier, M. F. & Preat, T. (2000). Ciboulot regulates actin assembly during Drosophila brain metamorphosis. *Cell*, **102**, 797–808.
22. Quinlan, M. E., Heuser, J. E., Kerkhoff, E. & Mullins, R. D. (2005). Drosophila Spire is an actin nucleation factor. *Nature*, **433**, 382–388.
23. Ahuja, R., Pinyol, R., Reichenbach, N., Custer, L., Klingensmith, J., Kessels, M. M. & Qualmann, B. (2007). Cordon-bleu is an actin nucleation factor and controls neuronal morphology. *Cell*, **131**, 337–350.
24. Valentijn, L. J., Koster, J. & Versteeg, R. (2006). Read-through transcript from NM23-H1 into the neighboring NM23-H2 gene encodes a novel protein, NM23-LV. *Genomics*, **87**, 483–489.
25. Kato, M., Khan, S., Gonzalez, N., O'Neill, B. P., McDonald, K. J., Cooper, B. J. *et al.* (2003). Hodgkin's lymphoma cell lines express a fusion protein encoded by intergenically spliced mRNA for the multilectin receptor DEC-205 (CD205) and a novel C-type lectin receptor DCL-1. *J. Biol. Chem.* **278**, 34035–34041.
26. Van Troys, M., Dewitte, D., Goethals, M., Carlier, M. F., Vandekerckhove, J. & Ampe, C. (1996). The actin binding site of thymosin beta 4 mapped by mutational analysis. *EMBO J.* **15**, 201–210.
27. Vancompernolle, K., Goethals, M., Huet, C., Louvard, D. & Vandekerckhove, J. (1992). G- to F-actin modulation by a single amino acid substitution in the actin binding site of actobindin and thymosin beta 4. *EMBO J.* **11**, 4739–4746.
28. Au, J. K., Olivares, A. O., Henn, A., Cao, W., Safer, D. & De La Cruz, E. M. (2008). Widely distributed residues in thymosin beta4 are critical for actin binding. *Biochemistry*, **47**, 4181–4188.
29. Domanski, M., Hertzog, M., Coutant, J., Gutsche-Perelroizen, I., Bontems, F., Carlier, M. F. *et al.* (2004). Coupling of folding and binding of thymosin beta4 upon interaction with monomeric actin monitored by nuclear magnetic resonance. *J. Biol. Chem.* **279**, 23637–23645.
30. Irobi, E., Aguda, A. H., Larsson, M., Guerin, C., Yin, H. L., Burtnick, L. D. *et al.* (2004). Structural basis of actin sequestration by thymosin-beta4: implications for WH2 proteins. *EMBO J.* **23**, 3599–3608.
31. Bosch, M., Le, K. H., Bugyi, B., Correia, J. J., Renault, L. & Carlier, M. F. (2007). Analysis of the function of Spire in actin assembly and its synergy with formin and profilin. *Mol. Cell*, **28**, 555–568.
32. Bao, L., Loda, M. & Zetter, B. R. (1998). Thymosin beta15 expression in tumor cell lines with varying metastatic potential. *Clin. Exp. Metastasis*, **16**, 227–233.
33. Hannappel, E. (2007). beta-Thymosins. *Ann. N.Y. Acad. Sci.* **1112**, 21–37.
34. Lambrechts, A., Van Troys, M. & Ampe, C. (2004). The actin cytoskeleton in normal and pathological cell motility. *Int. J. Biochem. Cell. Biol.* **36**, 1890–1909.
35. Kobayashi, T., Okada, F., Fujii, N., Tomita, N., Ito, S., Tazawa, H. *et al.* (2002). Thymosin-beta4 regulates motility and metastasis of malignant mouse fibrosarcoma cells. *Am. J. Pathol.* **160**, 869–882.
36. Sun, H. Q., Kwiatkowska, K. & Yin, H. L. (1996). beta-Thymosins are not simple actin monomer buffering proteins. Insights from overexpression studies. *J. Biol. Chem.* **271**, 9223–9230.
37. Koutrafouri, V., Leondiadis, L., Avgoustakis, K., Livaniou, E., Czarnecki, J., Ithakissios, D. S. & Evangelatos, G. P. (2001). Effect of thymosin peptides on the chick chorioallantoic membrane angiogenesis model. *Biochim. Biophys. Acta*, **1568**, 60–66.
38. Muller, C. S., Huff, T. & Hannappel, E. (2003). Reduction of thymosin beta4 and actin in HL60 cells during apoptosis is preceded by a decrease of their mRNAs. *Mol. Cell. Biochem.* **250**, 179–188.
39. Lee, S. H., Zhang, W., Choi, J. J., Cho, Y. S., Oh, S. H., Kim, J. W. *et al.* (2001). Overexpression of the thymosin beta-10 gene in human ovarian cancer cells disrupts F-actin stress fiber and leads to apoptosis. *Oncogene*, **20**, 6700–6706.
40. Hutchinson, L. M., Chang, E. L., Becker, C. M., Shih, M. C., Brice, M., DeWolf, W. C. *et al.* (2005). Use of thymosin beta15 as a urinary biomarker in human prostate cancer. *Prostate*, **64**, 116–127.
41. Abdulkadir, S. A. & Kim, J. (2005). Genetically engineered murine models of prostate cancer: insights into mechanisms of tumorigenesis and potential utility. *Future Oncol.* **1**, 351–360.
42. Blomme, T., Vandepoele, K., De Bodt, S., Simillion, C., Maere, S. & Van de Peer, Y. (2006). The gain and loss of genes during 600 million years of vertebrate evolution. *Genome Biol.* **7**, R43.
43. Larkin, M. A., Blackshields, G., Brown, N. P., Chenna, R., McGettigan, P. A., McWilliam, H. *et al.* (2007). Clustal W and Clustal X version 2.0. *Bioinformatics*, **23**, 2947–2948.
44. Van de Peer, Y. & De Wachter, R. (1994). TREECON for Windows: a software package for the construction and drawing of evolutionary trees for the Microsoft Windows environment. *Comput. Appl. Biosci.* **10**, 569–570.
45. Hannappel, E. (1986). One-step procedure for the determination of thymosin beta 4 in small tissue samples and its separation from other thymosin beta

4-like peptides by high-pressure liquid chromatography. *Anal. Biochem.* **156**, 390–396.
46. Spudich, J. A. & Watt, S. (1971). The regulation of rabbit skeletal muscle contraction. I. Biochemical studies of the interaction of the tropomyosin-troponin complex with actin and the proteolytic fragments of myosin. *J. Biol. Chem.* **246**, 4866–4871.
47. Brenner, S. L. & Korn, E. D. (1983). On the mechanism of actin monomer-polymer subunit exchange at steady state. *J. Biol. Chem.* **258**, 5013–5020.
48. Detmers, P., Weber, A., Elzinga, M. & Stephens, R. E. (1981). 7-Chloro-4-nitrobenzeno-2-oxa-1,3-diazole actin as a probe for actin polymerization. *J. Biol. Chem.* **256**, 99–105.
49. Safer, D. (1989). An electrophoretic procedure for detecting proteins that bind actin monomers. *Anal. Biochem.* **178**, 32–37.
50. Aguda, A. H., Xue, B., Irobi, E., Preat, T. & Robinson, R. C. (2006). The structural basis of actin interaction with multiple WH2/beta-thymosin motif-containing proteins. *Structure*, **14**, 469–476.
51. Weeds, A. G., Harris, H., Gratzer, W. & Gooch, J. (1986). Interactions of pig plasma gelsolin with G-actin. *Eur. J. Biochem.* **161**, 77–84.
52. Corpet, F. (1988). Multiple sequence alignment with hierarchical clustering. *Nucleic Acids Res.* **16**, 10881–10890.
53. Gouet, P., Courcelle, E., Stuart, D. I. & Metoz, F. (1999). ESPript: analysis of multiple sequence alignments in PostScript. *Bioinformatics*, **15**, 305–308.
54. Rudin, C. M., Engler, P. & Storb, U. (1990). Differential splicing of thymosin beta 4 mRNA. *J. Immunol.* **144**, 4857–4862.
55. Li, X., Zimmerman, A., Copeland, N. G., Gilbert, D. J., Jenkins, N. A. & Yin, H. L. (1996). The mouse thymosin beta 4 gene: structure, promoter identification, and chromosome localization. *Genomics*, **32**, 388–394.
56. Hsiao, H. L. & Su, Y. (2005). Identification of the positive and negative cis-elements involved in modulating the constitutive expression of mouse thymosin beta4 gene. *Mol. Cell. Biochem.* **272**, 75–84.
57. Varghese, S. & Kronenberg, H. M. (1991). Rat thymosin beta 4 gene. Intron-containing gene and multiple retroposons. *J. Biol. Chem.* **266**, 14256–14261.
58. Bao, L. & Zetter, B. R. (2000). Molecular cloning and structural characterization of the rat thymosin beta15 gene. *Gene*, **260**, 37–44.